The Viscous Effect in Power Capture of Bottom-Hinged Oscillating Wave Surge Converters

Chen-Chou Lin[*1], Yi-Chih Chow[2], Shiaw-Yih Tzang[3]

[*]*Department of Mechanical and Mechatronic Eng., National Taiwan Ocean University*
Keelung, Taiwan

[1]cclin@mail.ntou.edu.tw

[2]*Department of Systems Eng. and Naval Architecture, National Taiwan Ocean University*
Keelung, Taiwan

[2]ycchow@email.ntou.edu.tw

[3]*Dept of Harbor and River Engineering, National Taiwan Ocean University*
Keelung, Taiwan

[3]sytzang@mail.ntou.edu.tw

***Abstract*— The numerical simulations were conducted for Bottom-Hinged Oscillating Wave Surge Converters (BH-OWSCs) using the computational-fluid-dynamics (CFD) software FLOW-3D, and based on the wave climate of the offshore sea in northeast Taiwan, that is, 1.5 meters of wave height and 7 seconds of the wave period. The results were compared with that using the simulation toolbox for wave energy converter (WEC), WEC-Sim, which is a based on the potential-flow assumption. Therefore, the viscous effect of the fluid in the BH-OWSC problem can be elucidated. This paper investigated the power capture of the BH-OWSC with various parameters including flap width, flap thickness, flap density, and position of center of mass. The results showed that, on average, the viscous loss of fluid would reduce the capture factor (C_F) of the BH-OWSC by 19.1%.**

***Keywords*— Bottom-Hinged, Oscillating Wave Surge Converter, Wave energy converter, viscous effect, capture factor, WEC-Sim.**

I. INTRODUCTION

Wave energy accounts for the highest proportion of global ocean energy reserves, with 8000-80000 TWh per year, which is much higher than other energy resources in the oceans. Considering the costs due to installation, maintenance, power transmission cables, etc., wave energy converters (WECs) installed at nearshore waters, depth ranging from 10 to 20 meters, presumably are more promising. In addition, risks due to the extreme weather such as typhoon should always be considered for wave energy exploitation in Taiwan or East Asia seas. In response to the above-mentioned issues, Oscillating Wave Surge Converter (OWSC) is considered to be the top choice of WEC type for Taiwan mainly due to its survivability in extreme waves by submerging the flap into the water and securing it onto the seabed. According to Whittaker and Folly [1], OWSCs primarily respond to the horizontal acceleration of fluid, hence the design space of most promise is that where the wave force is maximized. As a result, the capture factor [1], also known as capture width ratio (CWR) in [2], increases with increasing flap width except the widest flap case where the flap starts to behave as a two-dimensional device. Babarit et al. [2] developed wave-to-wire numerical models to simulate multiple types of WEC including a Bottom-fixed oscillating flap (i.e. OWSC). The capture width ratios obtained in their simulations of OWSC range from 0.52 to 0.72, which is the highest among the various types of WECs. Chang et al. [3] were also concerned with the energy capture efficiency of an OWSC, and they analyzed the problem using the potential-flow-based 2-D linear wavemaker theory and SPH (Smoothed Particle Hydrodynamics) simulations. However, the simulation conditions were the ideal flow field (i.e. no viscosity, Incompressible, non-swirling). Flocard et al. [4] studied the power capture problem of bottom-hinged pitching cylinders by experimental testing approach. They adjusted the inertia of the device so as to modify its natural frequency, and to match the incoming wave frequency. The result showed that the method of inertia modification could result in an increase of capture factor by 70-100% for the larger regular waves, and a 15-25% increase in power capture when compared to a constant inertia configuration. Qiu et al. [5] conducted tests on bottom-hinged pendulum WEC model and showed that the ballast has a significant effect on the energy conversion absorption of the model and that the efficiency achieves the maximum of 68% in ballast cases.

From the previous research results, we realized that the WECs will behave differently with respect to energy capture efficiency for different densities, mass center positions, flap geometry (widths and thicknesses) given a specific wave climate. To obtain an in-depth knowledge about the effects of these parameters to the capture efficiency of an OWSC, we shall perform three-dimensional numerical simulations to OWSC of various geometric and inertial parameters using the CFD software package FLOW-3D [6]. The discussed parameters include the flap width (B), flap thickness (d), flap density (D) and vertical position of the flap's center of mass (CM) as shown in Figure 1. In [7], Bhinder et al. compared the potential time domain viscous (PTDV) model with the CFD model with respect to OWSC by adding the viscous damping term of the Morison equation, and a good agreement of CFD and PTDV model was observed for regular waves

condition. In the current research, we have compared the CFD results to the results of WEC-Sim [8] for a check of the curve trends, since the drag effect was not added into our WEC-Sim force model.

II. NUMERICAL MODELLING

A CFD software package, FLOW-3D [6], was used to perform numerical simulation of the OWSC. FLOW-3D is a RANS (Reynolds Averaged Navier-Stokes) equations solver, featuring so-called TruVOF to increase the accuracy of boundary conditions and the tracking of interfaces. In addition, a technique named FAVOR (Fractional Area Volume Obstacle Representation) method, is used to define general geometric regions within the rectangular grid. The above methods relieve the computation loading in calculating the dynamic boundary of the fluid-structure interface. A laminar fluid model was applied in the simulation.

A. Flap model

The investigated WEC device in the current research is a bottom-hinged oscillating wave surge converter (BH-OWSC). The flap's bottom hinge connects the flap to the seabed so that the flap can receive the wave force and then undergo a pitch motion to capture the wave's surge force/power. Figure 1 shows the shape and dimensions of the flap of an OWSC, where d denotes the flap thickness, B the flap width, CM the vertical distance of the center of mass to the hinge. The vertical distance between the still water surface to the hinge is 9 m (denoted by *l*), which is also defined as the flap height. The water depth (H) is 10 m.

As shown in Table 1, the design parameters include flap density (D), center of mass position (C_M), flap thickness (d), and flap width (B). The density of the flap is chosen to be 309 kg/m3 and 550 kg/m3. Two vertical positions of the center of mass are studied, one is $C_M = l/2$, indicating the flap body has a uniform mass distribution, and the other is $C_M = l/4$, implying a lower center of mass position or heavier mass at the flap's bottom portion. Three different flap thicknesses are studied, that is, 1 m, 2 m and 4 m, the corresponding flap thickness to wavelength ratios (d/L) are 1/60, 1/30, and 1/15, respectively. Two different flap widths are used, that is, 10 m and 20 m, the corresponding flap width to wavelength ratios (B/L) are 1/6 and 1/3, respectively. Here we adopt the characteristic wavelength of the northeast sea in Taiwan as the denominator, that is, L = 60 m, hence non-dimensional quantities d/L and B/L are used in the subsequent discussions.

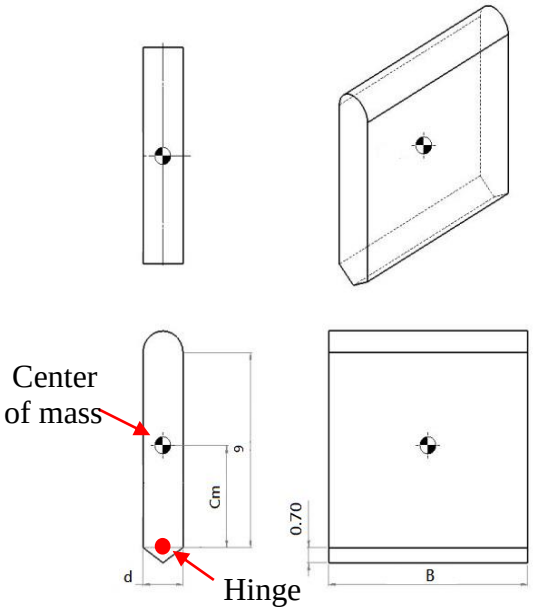

Fig. 1. The shape and dimensions of a flap

Table 1. The design parameters of the flap

Parameters	Quantity		
Flap density D (kg/ m^3)	309	550	
Vertical Position of center of mass C_M	*l*/2	*l*/4	
Flap thickness d (m)	1	2	4
Flap thickness to wavelength ratio d/L	1/60	1/30	1/15
Flap width B (m)	10	20	
Flap width to wavelength ratio B/L	1/6	1/3	

B. Computation domain and mesh setting

Since FLOW-3D uses a multi-block grid structure, here we used three mesh blocks to model the whole computation domain, as shown in Figure 2. The first block is the wave-forming area that allows the wave to travel 90 (180) meters (1.5 (3) times of wave lengths) before hitting the flap so that the wave can be formed completely. However, the 90-meters long wave forming area model was somewhat short, in which its reflected wave would hit the upwave boundary condition. Hence, we changed the block length to 180 meters. During the calculation of wave power absorption, we disregard the first two responding oscillations of the flap to avoid the incompletion during the wave forming. The second block is the wave-flap interaction area, which is 23 meters long. In this area, due to the interactions between the wave and the flap, there will be a drastic change in the movement of the flap. Therefore, the mesh size in this area was chosen to be two times finer than that of the first block. The fine grid can also describe the geometric shape of the moving flap more

accurately. The third block is the exit zone, where the mesh size is the same as that in the wave forming area. The fourth block is the wave dissipating area. In this 60-meter-long (one wave length) zone there is a numerical wave-dissipating scheme that allows the wave to be fully dissipated. There are two widths for the wave tank (W_{tank}), one is 100-meter for the wide flap model (B = 20 m) simulation, the other is 50-meter for the narrow flap model (B = 10 m) simulation. The ratio of the flap width to the wave tank width is kept at 1/5 to avoid the side-wall reflection effect.

The boundary conditions of the computation domain applied to the CFD simulation are shown in Figure 3. The inlet of the tank was specified as a wave boundary; the sides of the tank were specified as a symmetry boundary; the top boundary of the domain was specified as a pressure outlet with a fixed pressure; and the tank outlet was specified as an outflow boundary.

To find the appropriate mesh size of the simulation problem, four sets of mesh sizes were tested to find the effect of mesh resolution on the computation time and flap's response (angle of rotation). The mesh sizes are expressed as the ratio to the wavelength (L = 60 m), which are shown in details in Table 2. The first set of mesh size were most coarse one, with 23442 cells, and the angle of rotation was 25.5° . The angle of rotation computed based on the second, third and fourth sets of mesh size, were 27.42° , 27.72° and 27.86° , and the computation time were 5 mins, 53 mins, and 16 hrs, respectively. From the values of the flap's angle of rotation, it indicated that the response of the flap was converged. Based on the above, we then chose the third set (1/200 for the flap movement area, 1/100 for the rest area) as the primary mesh setting in this study. Figure 4 shows the third set of grid size in a snapshot of the computation domain.

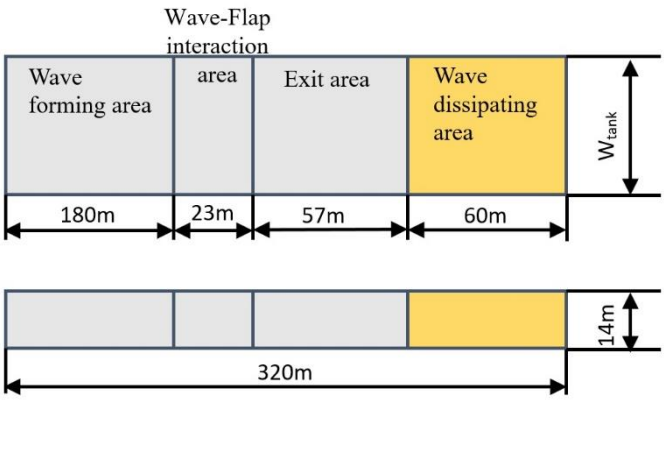

Fig. 2. The computation domain and mesh blocks, top and side view. (not in scale)

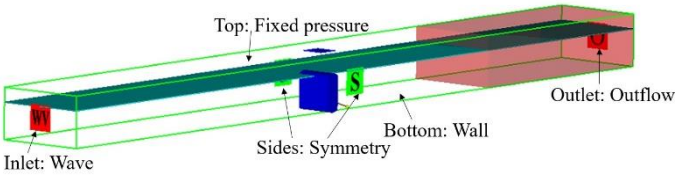

Fig. 3. The boundary conditions of the computation domain

Table 2. Convergence test for different mesh size. All mesh sizes are expressed in ratio to wavelength.

Flap movement area	Other Areas	Total Cells	Computation time	rotation angle (deg.)
1/60	1/30	23442	40 secs	25.5
1/120	1/60	149,730	5 mins	27.42
1/200	1/100	633,863	53 mins	27.72
1/400	1/200	10,291,081	16 hrs	27.86

C. Wave conditions

Linear wave was applied to the numerical simulation. The wave climate in the northeast sea of Taiwan, with a wave period of 7 seconds and wave height of 1.5 meters, was used as the wave condition in the current simulation. Given a 10 meters water depth, the wavelength of the linear wave was calculated to be 60 m based on the dispersion relation. Figure 5 shows a snapshot of the CFD simulation.

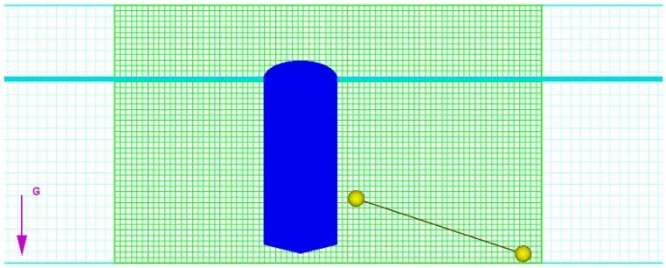

Fig. 4. The grid size of the third set of the mesh

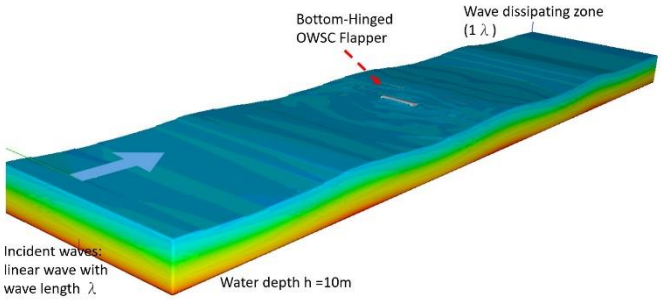

Fig. 5. The snapshot of the CFD simulation (FLOW-3D)

III. CAPTURE FACTOR

A. The model for capture factor function

Chang et al. [3, 9] had developed a 2-D analytical model for BH-OWSC based on potential flow assumption and wavemaker theory. In their formulations, the capture factor can be expressed as function of multiple non-dimensional mechanical impedances, including impedance resulting from wave field, PTO, and flap inertia properties. Assuming the 2-D resonance of the BH-OWSC is achieved, the capture factor can be expressed as

$$C_F = \frac{2P_3^*}{\left(1+P_3^*\right)^2} \tag{1}$$

C_F is a single-peak function starting from zero at $P_3^* = 0$ and asymptotically approaching zero as P_3^* approaches infinity, and where P_3^* denotes the normalized damping impedance of PTO, and can be expressed as

$$P_3^* = \frac{P_3}{W_1} = \left[\frac{1}{8\rho_w h^4}\right]\left(\frac{f_{PTO}}{\omega W_1}\right) \tag{2}$$

where f_{PTO} denotes the damping coefficient of the PTO in 2D version, ρ_w denotes the water density, h denotes the water depth, ω denotes the angular frequency of the wave, and W_1 denotes impedance associated with progressive waves, or the radiation damping effect, and can be expressed as

$$W_1 = \frac{\left(\int_{-1}^{0}\frac{\left(1+z^*\right)}{2}\cosh k_i^*\left(1+z^*\right)dz^*\right)^2}{k_i^*\int_{-1}^{0}\cosh^2 k_i^*\left(1+z^*\right)dz^*} = \frac{\left(k_i^*\sinh k_i^* - \cosh k_i^* + 1\right)^2}{\left(k_i^*\right)^4\left(2k_i^* + \sinh 2k_i^*\right)} \tag{3}$$

where $k_i^* = k_i h$ and $z^* = z/h$ are the non-dimensional wave number of the incident wave and z coordinate, respectively.

Chow et al. [10] further extend the methodology to 3D domain. Hence the capture factor can be expressed as

$$C_F = \frac{2\alpha_1 P_3^*}{\alpha_3 + \left(\alpha_2 + P_3^*\right)^2} \tag{4}$$

where α_1, α_2, represent functions in flap shape parameters, and α_3 represents the inertial effect of the flap on C_F.
In this paper, we adopted Eq. (4) as the model for curve fitting the simulation results.

IV. RESULTS

The following discussions focus on the effects of fluid viscosity to the capture factor of BH-OWSC under different flap geometric and inertia properties.

A. Comparison between FLOW-3D and WEC-Sim

Instead of using experimentation as the validation tool, here we compared the FLOW-3D simulation result to the reliable open source WEC simulation tool, WEC-Sim [8], whose computational architecture is based on rigid body dynamics simulation scheme. WEC-Sim is an open source wave energy converter simulator developed by National Renewable Energy Laboratory and Sandia National Laboratory. The preprocessor of WEC-Sim is a panel method based software, such as WAMIT or NEMOH, to compute the wave loads and motions of offshore structures in waves. The primary difference in our interest between WEC-Sim and the CFD software was that we did not add the viscous drag term into the force model of WEC-Sim, hence the results of WEC-Sim did not respond the viscous loss by the fluid, and the calculated capture factor values were presumably higher than those results from FLOW-3D. The capture factors curves resulted from the two software packages were compared. Further studies about the model with viscous drag effect will be conducted in a subsequent research using experimental method. Table 3 shows the difference of peak C_F values between the results from the two software packages.

Figure 6 shows the calculated C_F data and the fitting curves for the simulation case 1, where the curve pattern resulted from the two software packages are quite similar and the normalized PTO's damping impedances corresponding to the optimal C_F are very close, only that a difference between the optimal C_F of two curves exists. The difference between the curves is presumably resulted from the fluid viscous loss in the CFD model. For case 1, the difference between the two peaks (optimal C_F) is 43.9%, which is the greatest difference among the 24 cases.

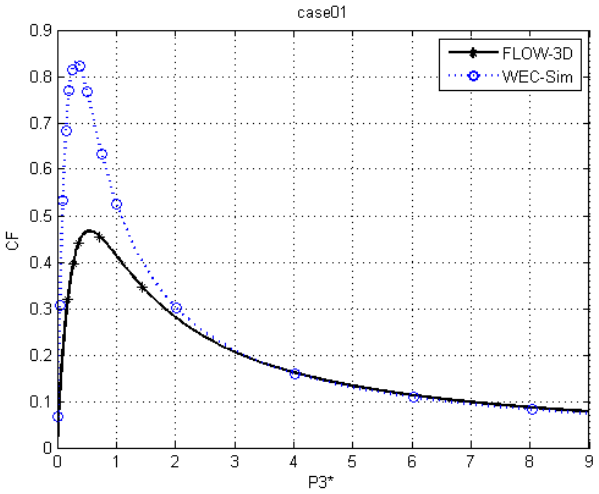

Fig. 6 C_F calculated data and fitting curves of simulation case 1 from FLOW-3D and WEC-Sim

Table 3 C_F results of FLOW-3D and WEC-Sim

Case no.	Flap density (D) (kg/m^3)	Center of mass position (C_M)	Flap thickness (d) (m)	Flap width (B) (m)	FLOW-3D C_F peak value (P1)	WEC-Sim C_F peak value (P2)	Difference $\frac{P2-P1}{P2}$
1	309	*l*/2	1	10	0.4667	0.8322	43.9%
2	309	*l*/2	1	20	0.4318	0.7361	41.3%
3	309	*l*/2	2	10	0.5924	0.7327	19.1%
4	309	*l*/2	2	20	0.6373	0.7988	20.2%
5	309	*l*/2	4	10	0.9834	0.9908	0.7%
6	309	*l*/2	4	20	0.7535	0.8931	15.6%
7	309	*l*/4	1	10	0.4936	0.6023	18.0%
8	309	*l*/4	1	20	0.6134	0.7393	17.0%
9	309	*l*/4	2	10	0.6976	0.8206	15.0%
10	309	*l*/4	2	20	0.6848	0.8297	17.5%
11	309	*l*/4	4	10	1.0013	1.2605	20.6%
12	309	*l*/4	4	20	0.7705	0.9391	17.9%
13	550	*l*/2	1	10	0.4333	0.7699	43.7%
14	550	*l*/2	1	20	0.5716	0.7186	20.5%
15	550	*l*/2	2	10	0.5425	0.6284	13.7%
16	550	*l*/2	2	20	0.5929	0.7629	22.3%
17	550	*l*/2	4	10	0.7807	0.7343	-6.3%
18	550	*l*/2	4	20	0.6617	0.8191	19.2%
19	550	*l*/4	1	10	0.4814	0.5789	16.8%
20	550	*l*/4	1	20	0.6085	0.7382	17.6%
21	550	*l*/4	2	10	0.6630	0.7532	12.0%
22	550	*l*/4	2	20	0.6514	0.8106	19.6%
23	550	*l*/4	4	10	0.9325	1.0421	10.5%
24	550	*l*/4	4	20	0.7075	0.9042	21.8%

Figures 6 to 9 show the capture factor curves resulted from FLOW-3D and WEC-Sim for cases 1, 2, 13, and 14, respectively. The four cases all have a flap thickness of 1m and center of mass position of *l*/2. The differences between the two peak values (optimal C_F) of the four cases are shown in Fig. 10, where the average difference is 37.4%.

Fig. 11 shows the differences between the two optimal C_Fs of cases 7, 8, 19, 20, with a flap thickness of 1m and center of mass position of *l*/4. The average difference is 17.4%.

Fig. 12 shows the differences between the two optimal C_Fs of cases 3, 4, 15, 16, with a flap thickness of 2m and center of mass position of *l*/2. The average difference is 18.8%.

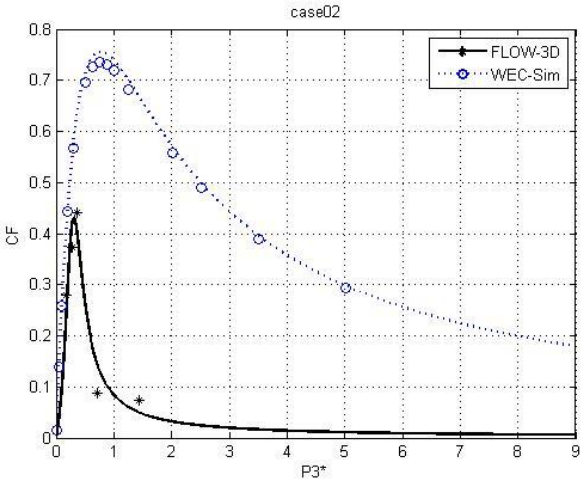

Fig. 7 C_F calculated data and fitting curves of simulation case 2 from FLOW-3D and WEC-Sim

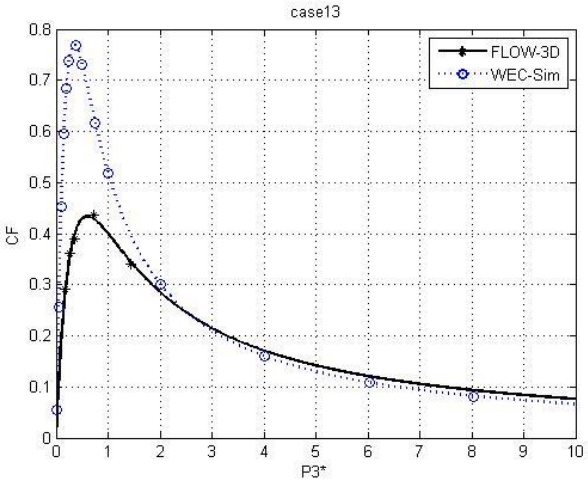

Fig. 8 C_F calculated data and fitting curves of simulation case 13 from FLOW-3D and WEC-Sim

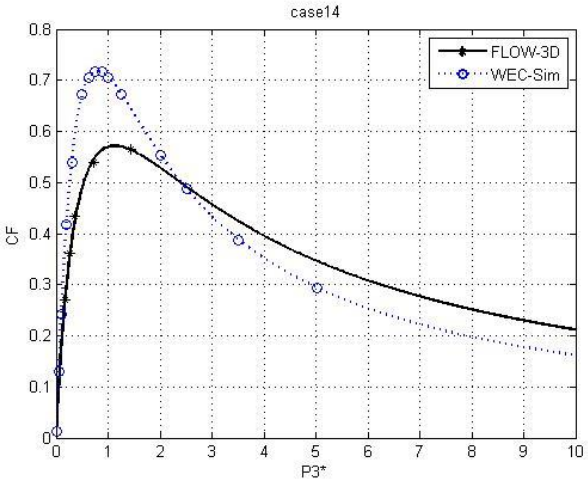

Fig. 9 C_F calculated data and fitting curves of simulation case 14 from FLOW-3D and WEC-Sim

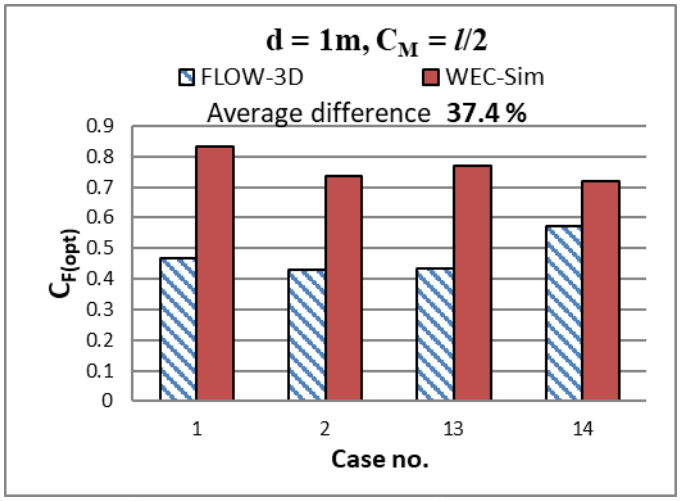

Fig. 10 The differences between the optimal C_{Fs} of FLOW-3D and WEC-Sim of cases 1, 2, 13, 14.

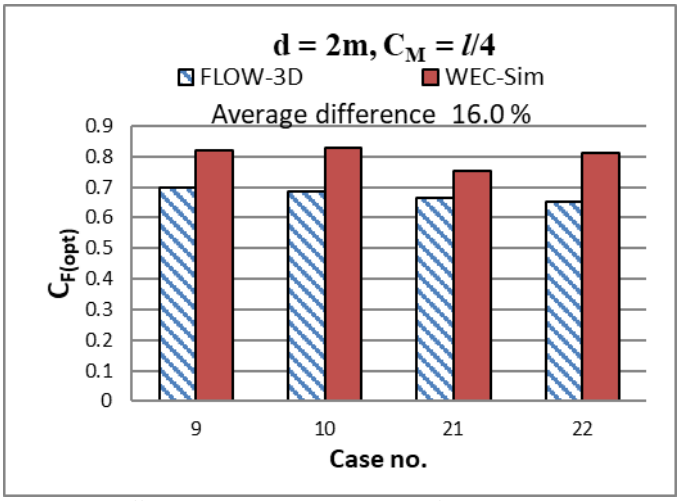

Fig. 13 The differences between the optimal C_{Fs} of FLOW-3D and WEC-Sim of cases 9, 10, 21, 22.

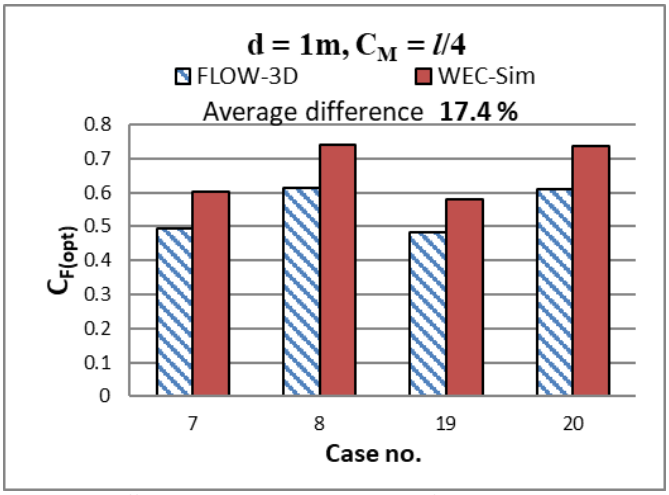

Fig. 11 The differences between the optimal C_{Fs} of FLOW-3D and WEC-Sim of cases 7, 8, 19, 20.

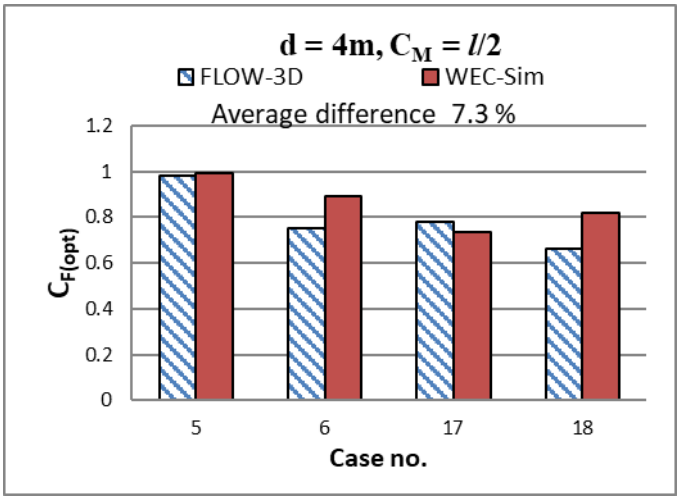

Fig. 14 The differences between the optimal C_{Fs} of FLOW-3D and WEC-Sim of cases 5, 6, 17, 18.

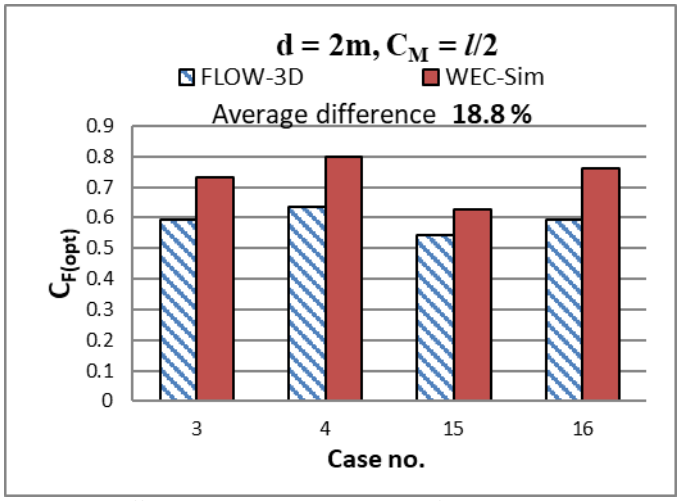

Fig. 12 The differences between the optimal C_{Fs} of FLOW-3D and WEC-Sim of cases 3, 4, 15, 16.

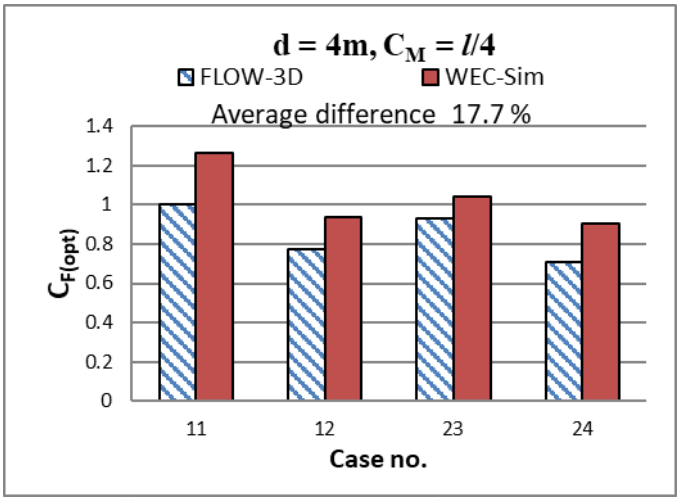

Fig. 5 The differences between the optimal C_{Fs} of FLOW-3D and WEC-Sim of cases 11, 12, 23, 24.

Fig. 13 shows the differences between the two optimal C_Fs of cases 9, 10, 21, 22, with a flap thickness of 2m and center of mass position of l/4. The average difference is 16%.

Fig. 14 shows the differences between the two optimal C_Fs of cases 5, 6, 17, 18, with a flap thickness of 4m and center of mass position of l/2. The average difference is 7.3%.

Fig. 15 shows the differences between the two optimal C_Fs of cases 11, 12, 23, 24, with a flap thickness of 4m and center of mass position of l/4. The average difference is 17.7%.

V. Conclusions

Instead of using experimentation as the validation tool, we compared the FLOW-3D simulation result to the open source WEC simulation tool, WEC-Sim, whose computational architecture is based on rigid body dynamics simulation scheme combined with hydrodynamic coefficients predicted by panel method. The difference between the fitted curves of the calculated data is presumably resulted from the fluid viscous loss in the CFD model. The results showed that

1. The calculated C_F data and the fitted curves for the 24 simulation cases show that the curve pattern resulted from the two software packages are quite similar and the normalized PTO's damping impedances corresponding to the optimal C_F are very close, only that a difference between the optimal C_F of two curves exists.
2. On average, the viscous loss of fluid would reduce the capture factor (C_F) of the BH-OWSC by 19.1%.
3. The greatest difference among the 24 cases between the optimal C_{Fs} of two software is 43.9%.
4. The four cases 1, 2, 13, 14, with flap thickness of 1m and center of mass position of l/2 has the greatest average optimal C_F difference of 37.4%.
5. The four cases 5, 6, 17, 18, with flap thickness of 4m and center of mass position of l/2 has the smallest average optimal C_F difference of 7.3%.
6. Among the four design parameters, flap thickness is most dominant in the viscous effect to C_F value. The flap with thickness 1m has the largest loss, while the flap with thickness 4m has the smallest loss.

Acknowledgment

The authors would like to thank the support of Ministry of Science and Technology of ROC Taiwan, under grant number MOST106-2221-E-019 -066.

References

[1] Trevor Whittaker, Matt Folley, Nearshore oscillating wave surge converters and the development of Oyster, Phil. Trans. R. Soc. A, 370, (2012), 345-364.

[2] A. Babarit, J. Hals, M.J. Muliawan, A. Kurniawan, T. Moan, J. Krokstad, Numerical benchmarking study of a selection of wave energy converters, Renew. Energy, 41 (2012) 44-63.

[3] Y.C. Chang, D.W. Chen, Y.C. Chow, S.Y. Tzang, C.C. Lin, J.H. Chen, Theoretical analysis and SPH simulation for the wave energy captured by a bottom-hinged OWSC, J. Mar. Sci. Technol.-Taiwan, 23 (2015) 901-908.

[4] F. Flocard, T.D. Finnigan, Increasing power capture of a wave energy device by inertia adjustment, Applied Ocean Research, 34 (2012), 126-134.

[5] S.Q. Qiu, J.W. Ye, D.J. Wang, and F.L. Liang, Experimental Study on A Pendulum Wave Energy Converter, China Ocean Eng., 27(3), (2013), 359-368.

[6] FLOW-3D Manual, V11.1, Flow Science Inc., Santa Fe, New Mexico, USA, 2017.

[7] M.A. Bhinder, A. Babarit, L. Gentaz, P. Ferrant, Potential time domain model with viscous correction and CFD analysis of a generic surging floating wave energy converter, International Journal of Marine Energy, 10 (2015) 70–96.

[8] WEC-Sim: The Open-Source Wave Energy Converter Simulator, User Guide, Version 3.0, National Renewable Energy Laboratory and Sandia National Laboratory.

[9] Y.C. Chang, Y.H. Lee, Y.C. Chow, C.C. Lin, S.Y. Tzang, J.H. Chen, Mechanical impedance effects on the capture factor of OWSC, J. Taiwan Soc. Nav. Archit. Mar. Eng. 33 (2014) 183-192. (in Chinese)

[10] Chow, Y.C., Y.C. Chang, D.W. Chen, C.C. Lin, S.Y. Tzang , 2018, Parametric Design Methodology for Maximizing Energy Capture of a Bottom-Hinged Flap-Type WEC with Medium Wave Resources, Renewable Energy, 126 (2018), 605-616.